JOURNAL OF BACTERIOLOGY, May 2011, p. 2290–2300 Vol. 193, No. 9
0021-9193/11/$12.00 doi:10.1128/JB.01555-10

Characterization of Mutants Deficient in the L,D-Carboxypeptidase (DacB) and WalRK (VicRK) Regulon, Involved in Peptidoglycan Maturation of *Streptococcus pneumoniae* Serotype 2 Strain D39▽†

Skye M. Barendt, Lok-To Sham, and Malcolm E. Winkler*

Department of Biology, Indiana University Bloomington, Bloomington, Indiana 47405

Received 28 December 2010/Accepted 18 February 2011

Peptidoglycan (PG) hydrolases play critical roles in the remodeling of bacterial cell walls during division. PG hydrolases have been studied extensively in several bacillus species, such as *Escherichia coli* and *Bacillus subtilis*, but remain relatively uncharacterized in ovococcus species, such as *Streptococcus pneumoniae* (pneumococcus). In this work, we identified genes that encode proteins with putative PG hydrolytic domains in the genome of *S. pneumoniae* strain D39. Knockout mutations in these genes were constructed, and the resulting mutants were characterized in comparison with the parent strain for growth, cell morphology, PG peptide incorporation, and in some cases, PG peptide composition. In addition, we characterized deletion mutations in nonessential genes of unknown function in the WalRK$_{Spn}$ two-component system regulon, which also contains the essential *pcsB* cell division gene. Several mutants did not show overt phenotypes, which is perhaps indicative of redundancy. In contrast, two new mutants showed distinct defects in PG biosynthesis. One mutation was in a gene designated *dacB* (*spd_0549*), which we showed encodes an L,D-carboxypeptidase involved in PG maturation. Notably, *dacB* mutants, similar to *dacA* (D,D-carboxypeptidase) mutants, exhibited defects in cell shape and septation, consistent with the idea that the availability of PG peptide precursors is important for proper PG biosynthesis. Epistasis analysis indicated that DacA functions before DacB in D-Ala removal, and immunofluorescence microscopy showed that DacA and DacB are located over the entire surface of pneumococcal cells. The other mutation was in WalRK$_{Spn}$ regulon gene *spd_0703*, which encodes a putative membrane protein that may function as a type of conserved streptococcal shape, elongation, division, and sporulation (SEDS) protein.

Streptococcus pneumoniae is a Gram-positive, aerotolerant anaerobe that colonizes the nasopharyngeal cavities of children and adults (22, 25, 64). Besides acting as a commensal, *S. pneumoniae* is a human opportunistic pathogen that causes several serious invasive diseases, including pneumonia, otitis media (ear ache), meningitis, and bacteremia (4, 33, 34, 40, 64). The peptidoglycan (PG) is an important component of the cell surface of all bacteria (reviewed in references 8, 61, 65–67, and 73) and is the target for several antibiotics, including β-lactam antibiotics and vancomycin, used to treat pneumococcal infections (55, 68). Notably, resistance of *S. pneumoniae* to β-lactam antibiotics is increasing at an alarming rate due to multiple amino acid changes in the pneumococcal penicillin binding proteins (PBPs) (13, 23, 33, 36, 72).

S. pneumoniae cells are shaped like elongated ellipsoids called ovococci that divide in parallel planes perpendicular to their long axis (35, 73). To achieve this shape, *S. pneumoniae* uses two modes of PG biosynthesis (see reference 73). Peripheral biosynthesis extends the PG from the middle of dividing cells to the equator of what will become the daughter cells, whereas septal biosynthesis creates the PG barrier between the two daughter cells. The high-molecular-weight PBPs, three of which carry out both transglycosylation and transpeptidation reactions (class A) and two of which are monofunctional transpeptidases (class B), seem to localize to the midcell region (73), but it is not known whether they form separate complexes that engage in the two modes of PG biosynthesis. The biochemical and physiological functions of the pneumococcal high-molecular-weight PBPs have been the subject of numerous studies (see references 24, 39, and 46).

At some point in the division process, murein hydrolases separate and remodel the PG of the dividing cells. Relatively little is known about the murein hydrolases whose activity is restricted to cell division. The PcsB protein is a leading candidate for a division hydrolase (Table 1) (1, 41, 42). PcsB contains a CHAP domain found in some phage and bacterial murein amidases and endopeptidases (Fig. 1) (2, 29, 56, 71). PcsB is a relatively abundant (~5,000 monomers per cell) protein whose function is essential, although bypass suppressors can be isolated (1; unpublished data). However, purified PcsB does not exhibit murein hydrolytic activity, nor does depletion of PcsB alter the composition of PG peptides (1, 41), suggesting that PcsB may act as a scaffolding protein, that its hydrolase activity depends strongly on cooperative interactions with a partner in the cell membrane, or both. The *pcsB* gene is positively regulated by the WalRK$_{Spn}$ (VicRK) two-component system (TCS) (Table 1) (41–43). WalRK TCSs maintain cell wall homeostasis and respond to cell wall stresses, such as antibiotics, in low-GC Gram-positive bacteria largely through regulation of genes encoding PG hydrolases (see references 9 and 70). The WalR$_{Spn}$ (VicR) response regulator is essential

* Corresponding author. Mailing address: Department of Biology, Indiana University Bloomington, Jordan Hall 142, Bloomington, IN 47405. Phone: (812) 856-1318. Fax: (812) 855-6705. E-mail: mwinkler@bio.indiana.edu.

† Supplemental material for this article may be found at http://jb.asm.org/.

▽ Published ahead of print on 4 March 2011.

TABLE 1. Genes encoding proteins with known or putative PG lytic domains and $WalRK_{Spn}$-regulated genes in *S. pneumoniae* serotype 2 strain D39

Gene or tag	Hydrolase class[a]	Domain name[b]	Cell morphology due to deletion mutation[e]	Relative growth of deletion mutant[e]	Relative PG peptide profile of deletion mutant[e]	Reference(s)
$WalRK_{Spn}$ regulon						
pcsB	Putative *N*-acetylmuramoyl-L-alanine amidase/endopeptidase	CHAP	Essential	None	WT[c] upon depletion	1, 42
lytB	*N*-Acetylglucosaminidase	Glucosaminidase	WT with slightly longer chains, very long chains when capsule is absent	WT	ND[d]	This work, 7, 15
spd_1874 (*spr1875*)	Putative *N*-acetylmuramidase	Mt3 hydrolytic	WT	WT growth rate and yield, slight lag when capsule is absent	WT	This work
spd_0703 (*spr0709*)	None (putative SEDS protein)	None	WT with aberrant incorporation of PG peptides	WT	WT	This work
spd_0104 (*spr0096*)	None (LysM domain)	None	WT	WT	ND	This work
Cell division						
pmp23	Putative lytic transglycosylase	PECACE	Aberrant cell morphology, i.e., long cells or large rounded cells within or at ends of chains, cell asymmetry	WT growth rate, decreased yield	WT	This work, 45, 47
dacA	D,D-Carboxypeptidase	Peptidase S11	Aberrant cell morphology, i.e., rounded cells, asymmetry, septal defects exaggerated when capsule is absent	Decreased growth rate and yield, lag	Aberrant	This work, 1, 38, 59
dacB (*spd_0549*; *spr0554*)	L,D-Carboxypeptidase	VanY/MEROPS M15 peptidase	Aberrant cell morphology, i.e., asymmetry, long chains, no chaining when capsule is absent	WT growth rate and yield and slight lag, slight decrease in growth rate and yield and slight lag when capsule absent	Aberrant	This work
Fratricide and autolysis during growth[d]						
lytA	*N*-Acetylmuramoyl-L-alanine amidase	Amidase_2	WT with infrequent cell asymmetry, slight chaining when capsule is absent	WT	ND	This work, 11, 18, 58
cbpD	Putative *N*-acetylmuramoyl-L-alanine amidase/endopeptidase	CHAP	WT	WT	WT	This work, 11, 12, 19, 26
lytC	*N*-Acetylmuramidase	Glyco_hydro_25	WT with slightly longer chains, slight chaining when capsule is absent	WT	WT	This work, 11, 20, 37, 48
Other putative hydrolases that do not affect cell division						
spd_0873 (*spr_0890*)	Putative *N*-acetylmuramidase	Glyco_hydro_25	WT	WT	ND	This work
spd_0173 (*spr_0168*)	Putative L,D-carboxypeptidase	Peptidase S66	WT	WT	ND	This work

[a] Based on reference 30.
[b] Determined using Pfam site (14).
[c] WT, phenotype similar to that of parent strain.
[d] ND, not determined.
[e] Determinations of growth properties, cell morphologies, and PG peptide compositions of deletion mutants were performed as described in Materials and Methods. PG peptide compositions upon depletion of PcsB and in Δ*pmp23* mutants were reported previously in references 1 and 45, respectively.

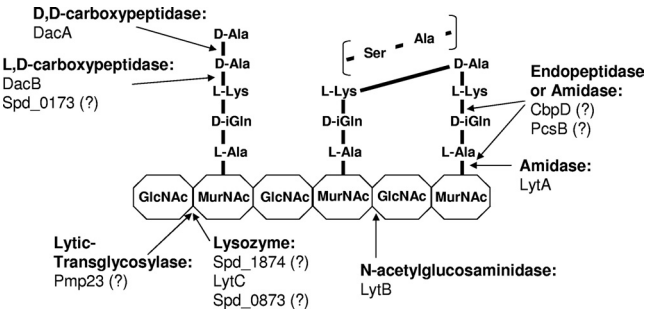

FIG. 1. Schematic diagram of one glycan strand of the pneumococcal PG showing proteins containing PG hydrolytic domains (see Table 1 and text) and known or putative sites of PG cleavage. Most interpeptide cross-links are direct in strain D39 (solid line between L-Lys and D-Ala) without the addition of L-Ser–L-Ala or L-Ala–L-Ala interpeptide cross bridges (see reference 1). PG hydrolase activities that have not been confirmed by biochemical analyses are indicated by question marks. MurNAc, *N*-acetylmuramic acid; GlcNAc, *N*-acetylglucosamine. Additional glycan strands, deacetylations and other modifications, and sites of attachment of capsule, teichoic acids, and proteins covalently linked by sortase are omitted for simplicity (see references 61 and 62).

through its positive regulation of *pcsB* (41, 42). Besides PcsB, the WalRK$_{Spn}$ regulon contains the LytB glucosaminidase that cleaves the PG glycan chain at a late step in cell division (Fig. 1) (7, 15, 32). The WalRK$_{Spn}$ regulon also encodes three other proteins of unknown function, including one putative lysozyme (Spd_1874) (Table 1; Fig. 1).

Besides PcsB, two other nonessential PG hydrolases, Pmp23 and DacA, were found to affect pneumococcal cell division and cell shape. Pmp23 encodes a membrane-bound PG hydrolase containing the recently described PECACE domain, which is confined to Gram-positive bacteria and may carry out lytic transglycosylase activity (Table 1; Fig. 1) (45, 47). DacA is a low-molecular-weight PBP that acts as a D,D-carboxypeptidase by cleaving the ultimate D-Ala from PG peptides (Fig. 1) (59, 66). DacA homologues are widely distributed in most bacterial species (17, 50, 53, 66). It has been proposed that DacA may regulate PBP transpeptidase cross-linking of the PG by limiting the amount and location of full-length PG pentapeptides containing D-Ala–D-Ala (38, 73). Finally, *S. pneumoniae* produces three PG hydrolases, LytA, CbpD, and LytC (Table 1; Fig. 1), that mediate the autolysis of stationary-phase cultures and the fratricide of noncompetent cells by competent cells (12, 32). These three hydrolases do not seem to play obligatory roles in pneumococcal cell division.

In this work, we identified genes that are predicted to encode additional PG hydrolases among the translated reading frames in the genome of serotype 2 strain D39 (28). We then constructed knockout mutations in each putative PG hydrolase gene, except for the essential gene *pcsB*, and in the genes for uncharacterized members of the WalRK$_{Spn}$ regulon in capsulated strain D39 and an isogenic unencapsulated derivative of strain D39. Characterization of these mutants led to the discovery of the L,D-carboxypeptidase, designated DacB (Table 1; Fig. 1), and its functional and spatial relationship to the DacA D,D-carboxypeptidase in *S. pneumoniae*. In addition, these findings implicate DacB and one member of the WalRK$_{Spn}$ regulon (Spd_0703) in cell division and confirm the previous conclusion that capsule influences pneumococcal cell shape and division properties (1).

MATERIALS AND METHODS

Bacterial strains and growth conditions. The strains used in this study are listed in Table 2. Bacteria were grown on plates containing Trypticase soy agar II (modified; Becton Dickinson) and 5% (vol/vol) defibrinated sheep blood (TSAII-BA) and incubated at 37°C in an atmosphere of 5% CO_2. Strains were cultured statically in Becton Dickinson brain heart infusion (BHI) broth at 37°C in an atmosphere of 5% CO_2, and growth was monitored by measuring optical density at 620 nm (OD_{620}) using a Spectronic 20 spectrophotometer fitted for measurement of capped tubes (outer diameter, 16 mm). Bacteria were inoculated into BHI broth from frozen cultures or colonies, serially diluted into the same medium, and propagated overnight. Overnight cultures that were still in exponential phase (OD_{620} = 0.1 to 0.6) were diluted back to an OD_{620} of 0.005 to start final experimental cultures, which did not contain antibiotics. In complementation experiments, final cultures contained 1% (wt/vol) fucose to induce the expression of wild-type genes controlled by the P_{fcsK} promoter in the ectopic *bgaA* site (Table 2) (5, 42).

Construction and verification of mutants. Strains containing antibiotic markers were constructed by transforming linear DNA amplicons synthesized by overlapping fusion PCR into competent pneumococcal cells as described previously (see references 42, 54, and 57). Primers synthesized for this study are listed in Table S1 in the supplemental material. Transformations were carried out as described before (42, 57). TSAII-BA plates were supplemented, as appropriate, with the following final concentration of antibiotic: 250 μg kanamycin per ml, 100 μg spectinomycin per ml, or 0.3 μg erythromycin per ml. All constructs were confirmed by PCR, where reaction mixtures contained genomic DNA prepared from cell lysates (5 μl of culture in 30 μl of 1× PCR buffer; heated for 10 min at 95°C) and KOD Turbo polymerase (Novagen). For key mutants (Δ*spd_0703*, Δ*dacB*, Δ*dacA*, Δ*pmp23*, and Δ*spd_1874*; Table 2), constructs were confirmed by DNA sequencing. Amplicons containing these mutations were purified using a PCR cleanup kit (Qiagen) and sequenced in reaction mixtures containing 1 μl of Big Dye Terminator reagent (Applied Biosystems) as described previously (28). Sequences were aligned and analyzed using Vector NTI software (Invitrogen).

Microscopy. Samples (100 μl) of cultures growing exponentially in BHI broth were taken at an OD_{620} of 0.15 to 0.35 and stained without fixation by adding 4,6-diamidino-2-phenylindole (DAPI) and a 1:1 mixture of vancomycin and Bodipy-FL-conjugated vancomycin (FL-Van; Molecular Probes) (51) to final concentrations of 0.2 and 2.0 μg/ml, respectively, for 10 min in the dark at room temperature. A 0.7-μl volume of broth culture or stained cells was added to a precleaned glass slide, a coverslip was added, and cells were examined using a Nikon E-400 epifluorescence phase-contrast microscope equipped with a mercury lamp, a 100 Nikon Plan Apo oil immersion objective (numerical aperture, 1.40), and filter blocks for fluorescence (DAPI, EX 330 to 380, DM 400, and BA 435 to 485; fluorescein isothiocyanate, EX 460 to 500, DM 505, and BA 510 to 560). Images were captured using a cooled digital Photometric CoolSnap HQ monochrome camera and processed with Nikon Elements AR software. In control experiments, cells in exponential phase (0.15 to 0.35) were examined without staining to ensure that cell morphology defects were not caused by vancomycin addition at these concentrations. Immunofluorescence microscopy (IFM) was performed by using commercially available polyclonal anti-FLAG antibody (Sigma F7425) as described in reference 69. Positive-control experiments showed proper localization of FLAG-tagged FtsZ at equators and septa (see reference 69), and negative-control experiments showed no detectable staining of bacteria that did not contain a FLAG-tagged protein (data not shown).

Preparation of cell-associated proteins, sodium dodecyl sulfate polyacrylamide gel electrophoresis (SDS-PAGE), and Western immunoblot analyses. Lysates were prepared from unencapsulated strains IU1945 (D39 Δ*cps*), IU4960 (D39 Δ*cps dacA*-L-FFF), and IU4961 (D39 Δ*cps dacB*-L-FFF) cultured in BHI broth to an OD_{620} of 0.2 to 0.3. One milliliter of each culture was microcentrifuged (21,000 × *g*, 10 min, 25°C), and cell pellets were resuspended in 100 μl of lysis buffer containing 40 μg mutanolysin (Sigma M9901) per ml as described in reference 69. Mixtures were incubated at 37°C for 10 min. A 100-μl volume of 2× SDS sample buffer (Bio-Rad 161-0737) containing 5% (vol/vol) β-mercaptoethanol (Sigma) was added to each sample, and the mixtures were incubated at 95°C for 10 min. Lysates were centrifuged at 3,400 × *g* for 3 min at 25°C, and 10-μl volumes of supernatants were resolved by 10% SDS-PAGE and then transferred to a nitrocellulose membrane as described in reference 1. Immunodetection was carried out using anti-FLAG polyclonal antibody (1:1,000 dilution; Sigma F7425), a donkey anti-rabbit secondary antibody conjugated with horseradish peroxidase (diluted 1:10,000; GE Healthcare NA934), and ECL detection

TABLE 2. Strains used in this study[a]

Strain	Genotype	Derivation	Antibiotic resistance[b]	Source(s)
EL59	Unencapsulated laboratory strain R6	Derived from intermediates of strain D39	None	28
EL556	R6 Δ*lytA*<>P$_c$-*aad9*	Δ*lytA*<>P$_c$-*aad9* × R6	Spec	57
IU1690	Serotype 2 capsulated D39	NTCC7466	None	28
IU1708	R6 Δ*cbpD*<>P$_c$-*kan-rpsL*	Δ*cbpD*<>P$_c$-*kan-rpsL* × EL59	Kan	This study
IU1732	R6 Δ*spd_1874*::*aad9* (3′ 27 nt[d] of *spd_1874* remain)	Δ*spd_1874*::*aad9* × EL59	Spec	This study
IU1945	D39 Δ*cps2A′*(*cps2BCDETFG*)*H′*	Δ*cps2A′*(*cps2BCDETFG*)*H′* × IU1690	None	28
IU2824	D39 Δ*dacA*<>P$_c$-*aad9*	Δ*dacA*<>P$_c$-*aad9* × IU1690	Spec	1
IU2825	D39 Δ*cps2A′*(*cps2BCDETFG*)*H′* Δ*dacA*<>P$_c$-*aad9*	Δ*dacA*<>P$_c$-*aad9* × IU1945	Spec	1
IU3766	D39 Δ*lytA*<>P$_c$-*aad9*	Δ*lytA*<>P$_c$-*aad9* × IU1690 (amplicon from EL556)	Spec	This study, 57
IU3775	D39 Δ*cbpD*<>P$_c$-*kan-rpsL*	Δ*cbpD*<>P$_c$-*kan-rpsL* × IU1690 (amplicon from IU1708)	Kan	This study
IU3795	D39 Δ*spd_1874*::*aad9* (3′ 27 nt of *spd_1874* remain)	Δ*spd_1874*::*aad9* × IU1690 (amplicon from IU1732)	Spec	This study
IU3797	D39 Δ*pmp23*<>P$_c$-*kan*	Δ*pmp23*<>P$_c$-*kan* × IU1690	Kan	This study
IU3800	D39 Δ*lytC*<>P$_c$-*kan-rpsL*	Δ*lytC*<>P$_c$-*kan-rpsL* × IU1690	Kan	This study
IU3801	D39 Δ*spd_0873*<>P$_c$-*kan-rpsL*	Δ*spd_0873*<>P$_c$-*kan-rpsL* × IU1690	Kan	This study
IU3804	D39 Δ*spd_0173*<>P$_c$-*kan-rpsL*	Δ*spd_0173*<>P$_c$-*kan-rpsL* × IU1690	Kan	This study
IU3805	D39 Δ*dacB*<>P$_c$-*kan-rpsL*	Δ*dacB*<>P$_c$-*kan-rpsL* × IU1690	Kan	This study
IU3806	D39 Δ*spd_0703*<>*kan*	Δ*spd_0703*<>*kan* × IU1690	Kan	This study
IU3837	D39 Δ*lytB*<>P$_c$-*kan-rpsL*	Δ*lytB*<>P$_c$-*kan-rpsL* × IU1690	Kan	This study
IU3874	D39 Δ*cps2A′*(*cps2BCDETFG*)*H′* Δ*cbpD*<>P$_c$-*kan-rpsL*	Δ*cbpD*<>P$_c$-*kan-rpsL* × IU1945 (amplicon from IU1708)	Kan	This study
IU3875	D39 Δ*cps2A′*(*cps2BCDETFG*)*H′* Δ*pmp23*<>P$_c$-*kan*	Δ*pmp23*<>P$_c$-*kan* × IU1945	Kan	This study
IU3876	D39 Δ*cps2A′*(*cps2BCDETFG*)*H′* Δ*lytC*<>P$_c$-*kan-rpsL*	Δ*lytC*<>P$_c$-*kan-rpsL* × IU1945	Kan	This study
IU3877	D39 Δ*cps2A′*(*cps2BCDETFG*)*H′* Δ*lytB*<>P$_c$-*kan-rpsL*	Δ*lytB*<>P$_c$-*kan-rpsL* × IU1945	Kan	This study
IU3878	D39 Δ*cps2A′*(*cps2BCDETFG*)*H′* Δ*spd_0873*<>P$_c$-*kan-rpsL*	Δ*spd_0873*<>P$_c$-*kan-rpsL* × IU1945	Kan	This study
IU3879	D39 Δ*cps2A′*(*cps2BCDETFG*)*H′* Δ*spd_0173*<>P$_c$-*kan-rpsL*	Δ*spd_0173*<>P$_c$-*kan-rpsL* × IU1945	Kan	This study
IU3880	D39 Δ*cps2A′*(*cps2BCDETFG*)*H′* Δ*dacB*<>P$_c$-*kan-rpsL*	Δ*dacB*<>P$_c$-*kan-rpsL* × IU1945	Kan	This study
IU3881	D39 Δ*cps2A′*(*cps2BCDETFG*)*H′* Δ*spd_0703*<>*kan*	Δ*spd_0703*<>*kan* × IU1945	Kan	This study
IU3900	D39 Δ*cps2A′*(*cps2BCDETFG*)*H′* Δ*lytA*<>P$_c$-*aad9*	Δ*lytA*<>P$_c$-*aad9* × IU1945 (amplicon from EL556)	Spec	This study, 57
IU3901	D39 Δ*cps2A′*(*cps2BCDETFG*)*H′* Δ*spd_1874*::*aad9* (3′ 27 nt of *spd_1874* remain)	Δ*spd_1874*::*aad9* × IU1945 (amplicon from IU1732)	Spec	This study
IU3917	D39 Δ*cps2A′*(*cps2BCDETFG*)*H′* Δ*spd_0104*<>P$_c$-*kan-rpsL* (5′ 30 nt and 3′ 30 nt of *spd_0104* remain)	Δ*spd_0104*<>P$_c$-*kan-rpsL* × IU1945	Kan	This study
IU3957	D39 Δ*cps2A′*(*cps2BCDETFG*)*H′* Δ*dacA*<>P$_c$-*aad9* Δ*dacB*<>P$_c$-*kan-rpsL*	Δ*dacB*<>P$_c$-*kan-rpsL* × IU2825	Spec, Kan	This study
IU4054	D39 *rpsL1* Δ*spd_0104*::P$_c$-*kan-rpsL* (5′ 30 nt and 3′ 30 nt of *spd_0104* remain)	Δ*spd_0104*<>P$_c$-*kan-rpsL* × IU1690	Kan	This study
IU4259	D39 Δ*dacB*<>P$_c$-*kan-rpsL* *bgaA*::P$_c$-*ermAM-P$_{fcsK}$-dacB*	*bgaA*::P$_c$-*ermAM-P$_{fcsK}$-dacB* × IU3805	Kan, Erm	This study
IU4787	D39 Δ*spd_0703*<>*kan* *bgaA*::P$_c$-*ermAM-P$_{fcsK}$-spd_0703*	*bgaA*::P$_c$-*ermAM-P$_{fcsK}$-spd_0703* × IU3806	Kan, Erm	This study
IU4960[c]	D39 Δ*cps2A′*(*cps2BCDETFG*)*H′* *dacA*-L-FFF	*dacA*$^+$-L-FFF-P$_c$-*aad9* × IU1945	Spec	This study
IU4961[c]	D39 Δ*cps2A′*(*cps2BCDETFG*)*H′* *dacB*-L-FFF	*dacB*$^+$-L-FFF-P$_c$-*kan* × IU1945	Kan	This study

[a] The genetic background was capsulated serotype 2 strain D39 (IU1690) or its isogenic unencapsulated derivative IU1945. Strains were constructed by transformation of amplicons (left of × sign) into the indicated recipient strain (right of × sign) as described in Materials and Methods. The symbols <> and :: indicate replacement of and insertion into a reading frame with an antibiotic marker, respectively.

[b] Antibiotic resistance markers: Erm, erythromycin; Kan, kanamycin; Spec, spectinomycin.

[c] L-FFF refers to a carboxyl-terminal addition of a 10-amino-acid spacer/linker (GSAGSAAGSG) followed by three tandem copies of the FLAG epitope (DYKDDDDK) (see reference 69).

[d] nt, nucleotides.

kits (Amersham) as described in reference 1. Autoradiography and quantitation using an IVIS imaging system were done as described before (1).

Determination of PG peptide composition. Bacteria were grown exponentially in BHI broth to an OD_{620} of 0.25 to 0.35. PG was extracted and PG lactoylpeptides were prepared and analyzed by high-performance liquid chromatography (HPLC), mass spectrometry (MS), and tandem MS as described previously (1).

RESULTS

Identification of genes encoding putative pneumococcal PG hydrolases and construction of isogenic mutants. New putative PG hydrolase genes listed in Table 1 were identified by searching the D39 genomic database (31) for Gram-positive PG hydrolytic domains described by Layec et al. (30) at the Pfam site (14). This compilation also contains *pmp23*, which encodes a putative lytic transglycosylase (Fig. 1) first identified and characterized in pneumococcal laboratory strain R6 (45). The list includes genes that are members of the $WalRK_{Spn}$ regulon, because the WalRK TCS has been shown to regulate numerous genes that mediate PG hydrolysis and remodeling in other low-GC Gram-positive species (see references 10, 66, and 70). Among the $WalRK_{Spn}$ regulon genes, *spd_1874* encodes a protein containing a LysM PG binding domain and a carboxyl mt3 hydrolytic domain found in PG-hydrolyzing (lysozyme) tape measure proteins of mycobacteriophage (3, 52). The regulon contains a second protein (Spd_0104) that contains the only other LysM domain in strain D39 but lacks a discernible hydrolase domain and a protein (Spd_0703) that contains two high-probability transmembrane domains separated by 3 amino acids, strongly suggesting localization of Spd_0703 in the membrane.

We constructed deletion-insertion mutations in each of the genes listed in Table 1. In most cases, we replaced entire reading frames with antibiotic resistance cassettes driven from constitutive promoters (Table 2). Because of concerns about polarity, the Δ*spd_0703* mutation contained a reading frame replacement lacking a constitutive promoter. Strong phenotypes of mutants were complemented by the expression of wild-type copies of genes from an ectopic site (see below; Table 2). Finally, we reported previously that the pneumococcal exopolysaccharide capsule influenced the cell shape and chaining characteristics of mutants (1). Consequently, we compared the effects of each mutation in isogenic sets of capsulated and unencapsulated strains derived from D39 (IU1690) and D39 Δ*cps* (IU1945), respectively (Table 2).

Δ*dacA*, Δ*pmp23*, Δ*dacB*, and Δ*spd_0703* mutations affect pneumococcal cell division and shape. Mutant strains were grown exponentially in BHI broth, and cell and chain morphologies were examined microscopically following staining with DAPI and fluorescent vancomycin (FL-V), which label DNA and regions of active PG biosynthesis marked by the presence of full-length PG pentapeptides containing D-Ala–D-Ala residues (Fig. 1) (1, 41, 42). Most of the mutants (Δ*lytB*, Δ*spd_1874*, Δ*spd_0104*, Δ*lytA*, Δ*cbpD*, Δ*lytC*, Δ*spd_0873*, and *spd_0173*) maintained wild-type cell morphology and growth rates (Table 1; data not shown). Three mutants, Δ*lytB*, Δ*lytA*, and Δ*lytC*, showed chaining similar to that of the capsulated parent strain. In the unencapsulated background, absence of the autolysins encoded by *lytA* and *lytC* caused slight increases in chaining compared to that of the parent (Table 1), whereas the unencapsulated Δ*lytB* mutant formed extremely long chains of cells, similar to those first reported for unencapsulated laboratory strain R6 (15). Thus, the presence of capsule mediated the chaining properties of some hydrolase mutants, consistent with our previous observations (1).

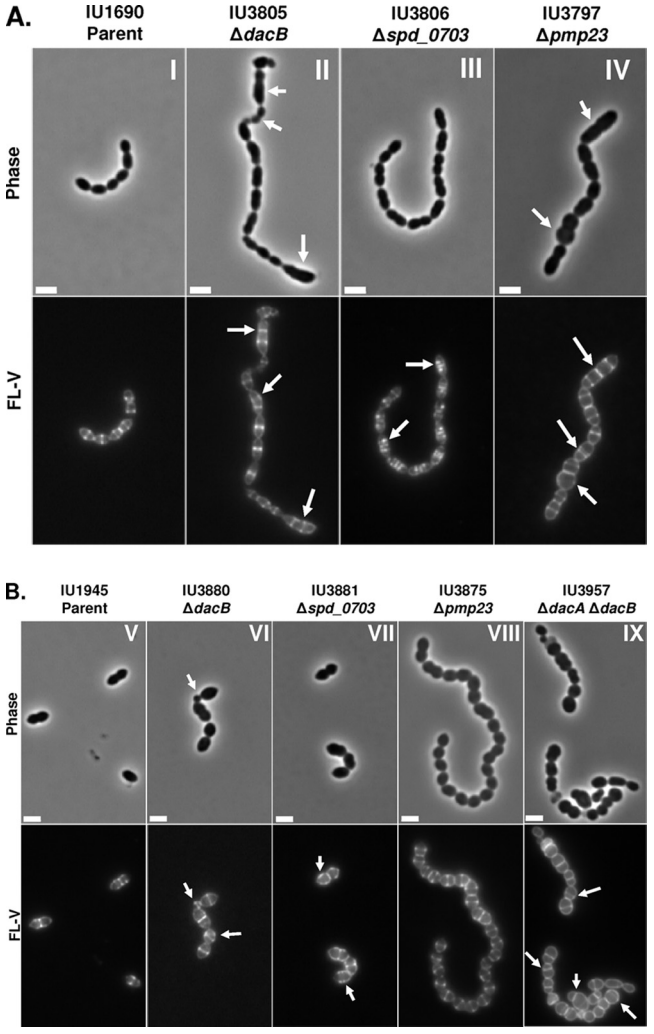

FIG. 2. Representative phase-contrast micrographs (top rows) and FL-V staining (bottom rows) of deletion mutants lacking PG hydrolases or $WalRK_{Spn}$ regulon members. Labeling and microscopy were carried out numerous times using independent cultures as described in Materials and Methods. (A) Deletion mutants in encapsulated strain D39: panel I, parent (IU1690); panel II, Δ*dacB* (IU3805); panel III, Δ*spd_0703* (IU3806); panel IV, Δ*pmp23* (IU3797). (B) Deletion mutants in isogenic unencapsulated strain D39: panel V, D39 Δ*cps* parent (IU1945); panel VI, Δ*dacB* (IU3880); panel VII, Δ*spd_0703* (IU3881); panel VIII, Δ*pmp23* (IU3875); panel IX, Δ*dacA* Δ*dacB* (IU3957). Arrows indicate defects in cell morphology (phase micrographs) or PG pentapeptide localization (FL-V micrographs) compared to the IU1690 or IU1945 parent strain. The scale bars correspond to 2 μm.

Notably, four mutants, Δ*dacA*, Δ*pmp23*, Δ*dacB*, and Δ*spd_0703*, showed severe defects in some aspect of cell morphology or division (Fig. 2 and 3). The decreased growth and yield, rounded cell shape, division asymmetry, and aberrant FL-V staining pattern of Δ*dacA* mutants have been reported previously in laboratory strain R6 and capsulated and unen-

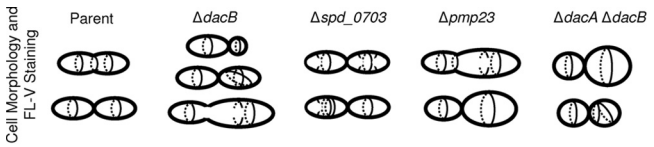

FIG. 3. Schematic summary of cell morphology and FL-V staining defects observed in mutants lacking PG hydrolases or WalRK$_{Spn}$ regulon members relative to the parent strain. Defects in cell shape and size are traced by peripheral lines, and hashed and solid lines near the middles of cells indicate equatorial, septal, and misplaced rings, ring segments, and puncta that were stained with FL-V. This summary is based on numerous images from independent cultures of each capsulated and unencapsulated mutant (see Fig. 2).

capsulated strain D39 (1, 38, 59) and are not recapitulated here, except in the context of Δ*dacB* mutants (see below).

In the D39 background, the growth rates of Δ*pmp23* mutants were similar to those of their parent strains but the mutants reproducibly had growth yields lower than those of their parents and autolyzed immediately upon entry into stationary phase, especially in the unencapsulated D39 strain (see Fig. S1 in the supplemental material). Cells in chains of capsulated D39 Δ*pmp23* mutants were larger than those of the parent and were frequently long and thick or bulbous and round. The round cells had occasional double septa and circumferential FL-V staining (Fig. 2A, panel IV, arrows, and 3). These aberrant cells resembled those reported previously for a small subpopulation of a Δ*pmp23* mutant of strain R6 (45). The shape and division defects of Δ*pmp23* mutants in the D39 background partly depended on capsule and were less pronounced in the unencapsulated background (compare Fig. 2A, panel IV, with B, panel VIII). Unencapsulated D39 Δ*pmp23* cells formed chains, in contrast to their diplococcal parent (Fig. 2B). This phenotype contrasts with the lack of chaining reported previously for *pmp23* mutants in laboratory strain R6 (45). Cells of unencapsulated Δ*pmp23* mutants again were somewhat rounded and occasionally round and bulbous, especially at ends of chains, compared to their parent. We confirmed these phenotypes of unencapsulated Δ*pmp23* mutants in three independent isolates containing different kinds of Δ*pmp23* mutations (data not shown). During the construction of these Δ*pmp23* mutants, there was no delay in the initial appearance of mutant colonies following transformation. Thus, it is unlikely that the less severe phenotype of the unencapsulated Δ*pmp23* mutants was caused by accumulation of suppressor mutations.

The division defects of the Δ*dacB* and Δ*spd_0703* mutants have not been reported before. *dacB* (*spd_0549*) was annotated as a putative D,D- or L,D-carboxypeptidase containing a VanY-like hydrolase domain (Table 1). The growth of Δ*dacB* mutants was similar to that of the capsulated or unencapsulated parent strains, except for a slightly lowered growth yield seen in the unencapsulated strain (see Fig. S1 in the supplemental material). Yet, capsulated or unencapsulated Δ*dacB* mutant cells showed extensive division asymmetry, indicated by the presence of very small, round cells and long, thick cells (Fig. 2A, panel II, B, panel VI, and 3). We hypothesized that if *dacB* encodes a D,D-carboxypeptidase, then FL-V staining should be similar to that of *dacA* mutants, which form spherical cells with strong peripheral staining and misplaced division planes (Fig. 2B, panel IX, and 3) (1). However, FL-V staining of Δ*dacB* mutants was largely confined to septa and equators, similar to the pattern of the parent strain (Fig. 2A and B). In addition, Δ*dacB* cells contained mislocalized septal rings and regions of staining, especially in elongated cells or cells with other morphological defects (Fig. 2A and B, arrows, and 3). Importantly, the morphological and division defects of Δ*dacB* mutants were completely complemented by expression of the *dacB*$^+$ gene from an ectopic site (see Materials and Methods; data not shown).

Δ*spd_0703* mutants exhibited normal growth, cell shape, chaining properties, and PG peptide composition compared to those of the parent strains (Table 1; Fig. 2). However, staining with FL-V revealed that many Δ*spd_0703* cells had additional discrete stained or broadened equatorial puncta of relatively similar intensities in both the capsulated and unencapsulated backgrounds (arrows, Fig. 2A, panel III, B, panel VII, and 3). This result suggests that the absence of Spd_0703 caused aberrant localization of PG pentapeptides containing D-Ala–D-Ala residues on cell surfaces. The aberrant FL-V staining of Δ*spd_0703* mutants was completely complemented by expression of the *spd_0703*$^+$ gene from an ectopic site (see Materials and Methods; data not shown).

DacB acts as an L,D-carboxypeptidase. Since the FL-V staining pattern of Δ*dacB* mutants did not match that of a mutant deficient in a D,D-carboxypeptidase, we hypothesized that DacB is an L,D-carboxypeptidase based on its predicted VanY-like hydrolase domain (Table 1) and homology to an L,D-carboxypeptidase previously identified in *Lactococcus lactis* (6). An enzyme with this hydrolytic activity (Fig. 1) was anticipated by the presence of linear, tripeptide PG monomers (M1, Fig. 4A, left panel) in the PG of *S. pneumoniae* D39 (1, 16). To test this idea, we compared the composition of the PG lactoyl-peptides from the unencapsulated Δ*dacB* mutant (IU3880) with that of the parent D39 Δ*cps* strain (Fig. 4A; see Materials and Methods). We found that the tripeptide PG monomer (M1) eluting at ~18 min decreased in relative amount from 18.6% ± 1.5% in the parent strain to 1.6% ± 0.03% in the Δ*dacB* mutant (Fig. 4A and C). Concomitantly, the tetrapeptide PG monomer (M2) eluting at ~35 min increased in relative amount from 1.3% ± 1.1% in the parent strain to 36.2% ± 1.0% in the Δ*dacB* mutant (Fig. 4A and C). The identities of the M1 and M2 species were confirmed by tandem MS analysis (Fig. 4B; see Materials and Methods). The Δ*dacB* mutation also caused accumulation of the D(*dacB*) tetramer-tetramer PG dimer (Fig. 4A, right panel), which eluted at about the same time as the major D1 tetramer-trimer PG dimer from the parent strain (Fig. 4A, left panel). The appearance of D(*dacB*), which contains an extra D-Ala residue, supports the conclusion that DacB is an L,D-carboxypeptidase that hydrolyzes the peptide bond between L-Lys and D-Ala at the fourth position in pneumococcal PG peptides (Fig. 1). In addition, the absence of DacB decreased the relative level of PG cross-linking. More D1 than D(*dacB*) was present (Fig. 4C), and the total relative amount of PG dimers plus trimers was greater in the *dacB*$^+$ parent (52.9% ± 4.8%) than in the Δ*dacB* mutant (35.9% ± 1.7%; Fig. 4A). This observation suggests that the M1 tripeptide PG monomer was the preferred substrate for the PBP transpeptidases rather than the M2 tetramer PG monomer.

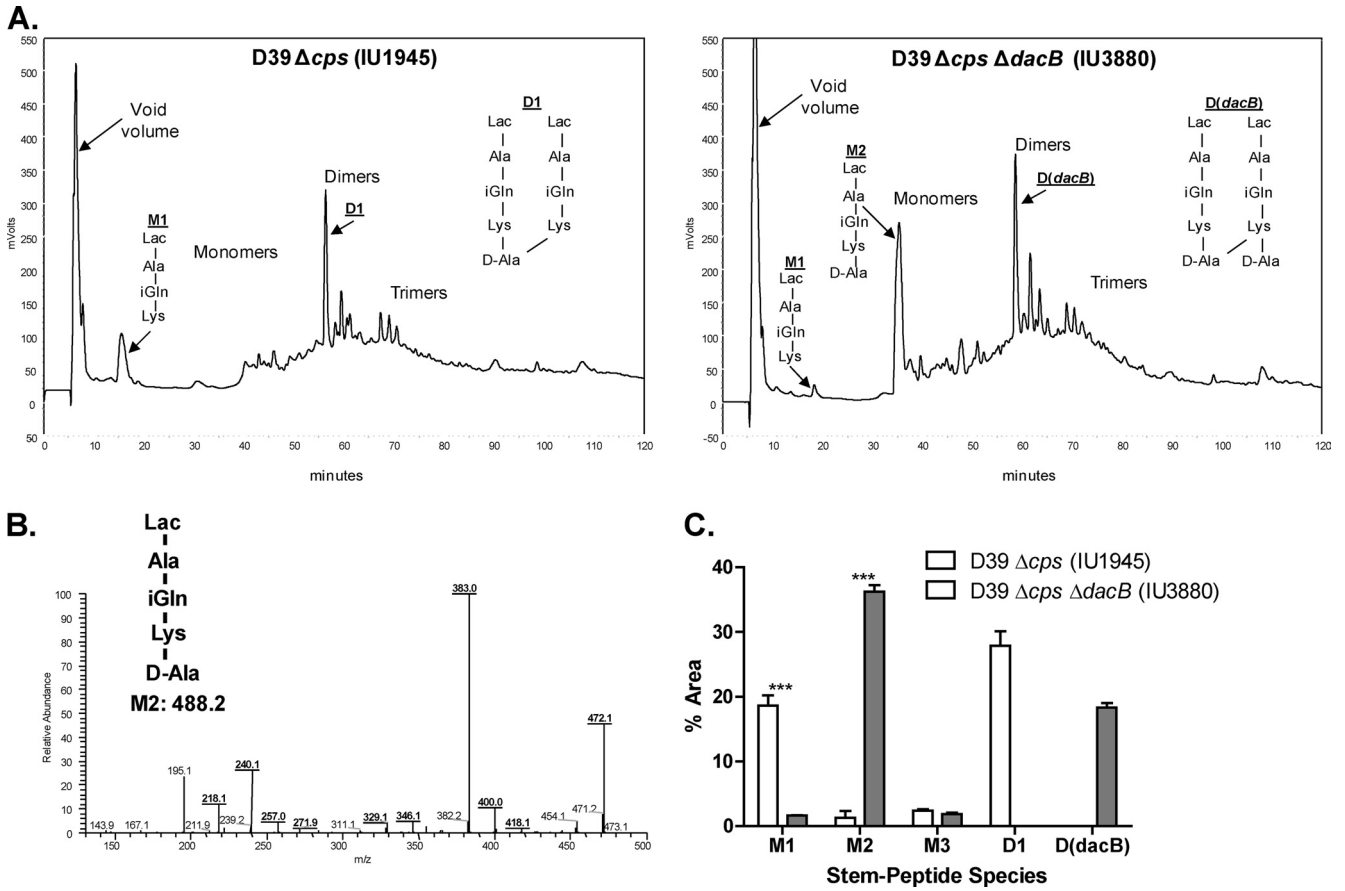

FIG. 4. Analyses of PG peptide composition in a Δ*dacB* mutant growing exponentially in BHI broth. PG was purified and hydrolyzed to lactoyl-peptides, which were resolved by reverse-phase HPLC and quantitated by measurement of A_{202} (see Materials and Methods) (1). (A) Representative reverse-phase HPLC chromatograms showing lactoyl-peptides from unencapsulated parent IU1945 (left panel) or isogenic Δ*dacB* mutant IU3880 (right panel). Peak assignments for strain IU1945 were determined previously (1), and those for the M1, M2, and D(*dacB*) species from strain IU3880 were determined directly by tandem MS (see below). Reverse-phase HPLC analyses were done at least three times independently for each strain. (B) Structure determination of the M2 tetrapeptide PG monomer from strain IU3880 (expected m/z = 488.2; actual m/z = 489.3) by tandem MS analysis (see reference 1). The fragmentation pattern corresponds to the following species, consistent with the M2 structure: m/z 472.1 (Lac-A-Q-K-A minus an NH_3 molecule), m/z 383.0 (Lac-A-Q-K minus an NH_3 molecule), and m/z 240.1 (internal fragment Q-K minus an NH_3 molecule). The identities of the M1 and D(*dacB*) species were determined by similar analyses (data not shown). (C) Comparison of the relative amounts of the M1 and M2 species in the parent and the Δ*dacB* mutant. Relative amounts of M1 and M2 were determined from the areas of peaks in each chromatogram as a percentage of the total area of all PG peptides (see reference 1). Relative amounts are averages from at least three independent experiments, and triple asterisks indicate differences at $P < 0.001$ in two-tailed t tests. For comparison, the average relative amounts of D1 and D(*dacB*) (see structures in panel A) in the parent and Δ*dacB* mutant strains, respectively, are shown.

Δ*dacA* is epistatic to Δ*dacB*. Epistasis of DacA function over DacB function was shown in two different ways. Δ*dacA* mutants accumulated the pentapeptide PG monomer M3 (relative amount = 32.5% ± 0.9%), which eluted at ~40 min in HPLC chromatograms (Fig. 1 and 5, inset). The PG peptide composition of the Δ*dacA* Δ*dacB* double mutant (Fig. 5) resembled that of the Δ*dacA* single mutant (Fig. 5, inset), rather than the Δ*dacB* single mutant (Fig. 4A). Notably, the Δ*dacA* and Δ*dacA* Δ*dacB* mutants accumulated the M3 PG pentapeptide but had minimal amounts of the M1 and M2 species. The identities of these peptides were confirmed by tandem MS analysis (data not shown). Thus, in the absence of the DacA D,D-carboxypeptidase, the DacB L,D-carboxypeptidase did not function, consistent with a sequential hydrolysis pathway in which DacA functions before DacB. This conclusion was supported by comparisons of cell morphology and FL-V staining of Δ*dacA*, Δ*dacB*, and Δ*dacA* Δ*dacB* mutants (Fig. 2B). Δ*dacA* and Δ*dacA* Δ*dacB* mutant cells had the same aberrant appearance (Fig. 2B, panel IX), which differed from that of the Δ*dacB* mutant (Fig. 2B, panel VI). This result is consistent with a lack of DacB L,D-carboxypeptidase function in the absence of DacA D,D-carboxypeptidase function.

DacA and DacB localize over the entire surface of pneumococcal cells. A previous study using laboratory strain R6 concluded that DacA localized everywhere in the *S. pneumoniae* cell, except for equators at the start of the cell division cycle (38). As peripheral and septal PG biosynthesis commenced (see introduction), DacA became localized somewhat amorphously in midcell regions. We localized DacA by IFM of an unencapsulated derivative of strain D39 (see Materials and

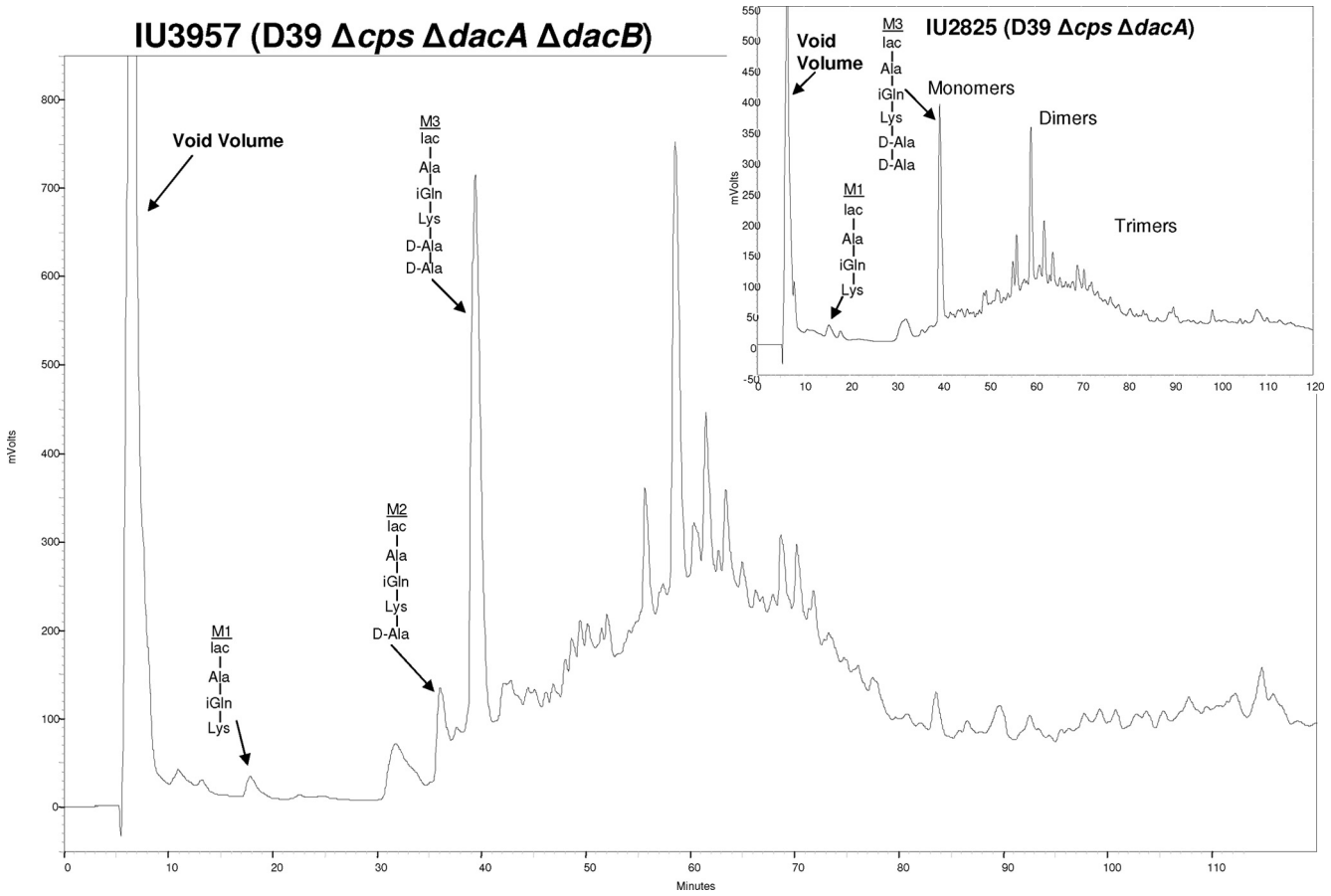

FIG. 5. PG lactoyl-peptide profile of Δ*dacA* Δ*dacB* double mutant IU3957 compared to that of Δ*dacA* single mutant IU2825 in the unencapsulated derivative of strain D39. Bacteria were growing exponentially in BHI broth at the time of sampling. The identities of the labeled M1 tripeptide, M2 tetrapeptide, and M3 pentapeptide were confirmed by tandem MS analysis (data not shown; see Fig. 4).

Methods) (69) (Fig. 6A). DacA expressed from its native chromosomal locus was epitope tagged at its carboxyl terminus with a linker (L) and three tandem copies of the FLAG tag (FFF) (Table 2) (69). The DacA-L-FFF construct was active, because we did not detect any defects in cell morphology characteristic of *dacA* mutants (e.g., see Fig. 2B, panel IX). Western blot assays showed a single band with a mass corresponding to that of full-length DacA-L-FFF and no shorter bands indicative of cleaved DacA-L-FFF species (data not shown). In addition, quantitative real-time PCR confirmed that the relative amount of transcript expressing DacA-L-FFF (or DacB-L-FFF; see below) was comparable to that expressing DacA (or DacB) in the wild-type parent strain (data not shown). Consistent with the previous result obtained with laboratory strain R6, DacA was located over entire peripheral surfaces of cells in all stages of separation (Fig. 6A). But in contrast to the previous report (38), we did not detect any clear gaps lacking DacA at the equators of nondividing cells or in cells at early stages of division. In addition, DacA was concentrated at the septa of some constricting cells (arrows, Fig. 6A4). Similar localization experiments were performed for DacB-L-FFF expressed from its native chromosomal locus (Fig. 6B). Again, cells expressing DacB-L-FFF did not show defects in morphology (e.g., see Fig. 2B, panel VI) and only a single band with a mass corresponding to DacB-L-FFF was detected in Western blot assays (data not shown). Like DacA, DacB was localized over the entire surface of cells at all stages of cell separation and at the septa of some constricting cells (arrows, Fig. 6B4).

DISCUSSION

The roles of PG hydrolases are poorly understood in *S. pneumoniae*, and previous phenotypic comparisons have not been done with an isogenic strain set. We report here that besides the essential PcsB protein (1, 41, 42), four proteins that are involved in or possibly associated with PG hydrolysis (Pmp23, DacA, DacB, and Spd_0703; Fig. 1) have marked effects on pneumococcal cell shape and division. On the other hand, as has been seen for other bacterial species (reviewed in reference 66), several putative pneumococcal hydrolases are not essential and may have redundant functions that are not revealed by single mutations (Table 1). For example, the Δ*spd_1874* single mutant showed normal growth, cell morphology, and PG peptide composition (Table 1). However, replacements of conserved amino acids in the putative lysozyme active site of Spd_1874 abolished some forms of bypass suppression of Δ*pcsB* deletions, suggesting that Spd_1874 likely acts as a lysozyme (unpublished data). Further analyses of combina-

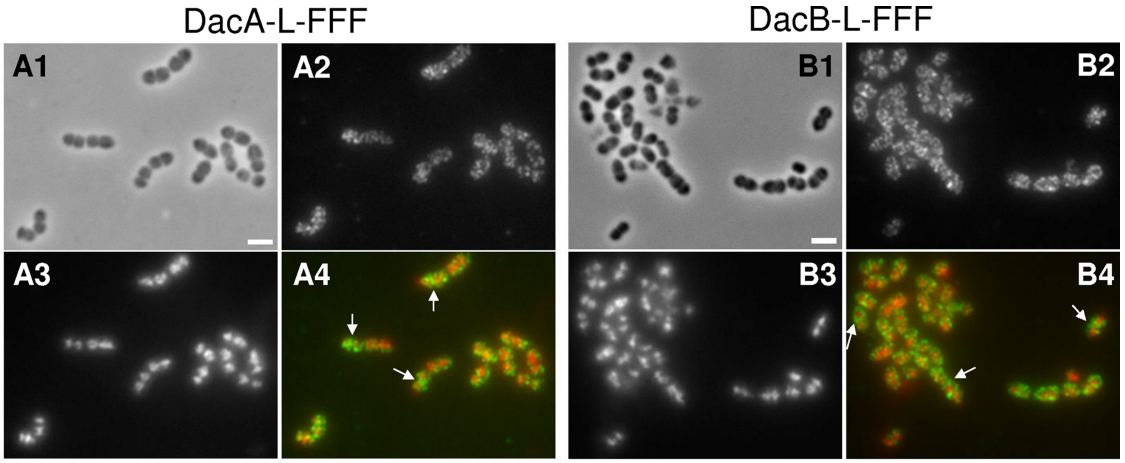

FIG. 6. IFM localization of $DacA_{Spn}$-L-FFF and $DacB_{Spn}$-L-FFF proteins in unencapsulated D39 pneumococcal cells growing exponentially in BHI broth. Strains IU4960 (A) and IU4961 (B) expressed $DacA_{Spn}$-L-FFF and $DacB_{Spn}$-L-FFF, respectively, from their native chromosomal loci, where L is a linker segment and FFF is three tandem copies of the FLAG epitope tag (see Materials and Methods; Table 2) (see reference 69). A1 and B1, phase-contrast micrographs; A2 and B2, IFM using polyclonal anti-FLAG antibody; A3 and B3, DAPI staining of nucleoids; A4 and B4, pseudocolored overlay, with IFM and DAPI staining colored green and red, respectively. Control IFM experiments showed no staining of cells lacking proteins fused to the FLAG tags (data not shown). The experiment was repeated independently and gave the same results. The arrows in panels A4 and B4 indicate septal localization of DacA and DacB, respectively, in some cells.

tions of the mutations in the genes in Table 1 may indicate functional and genetic redundancy and interactions (44, 63).

This study also confirmed and extended the previous conclusion that capsule exopolysaccharide influences the cell size and shape exhibited by division mutants (Fig. 2) (1). As expected from previous work (11, 19, 58), the PG autolysins LytA, LytC, and CbpD did not play obligatory roles in normal cell division and had marginal roles in chaining and cell separation in the absence of capsule (Table 1). The Δ*lytB* and Δ*pmp23* mutants exhibited more striking examples of the influence of capsule on division phenotypes (Table 1; Fig. 2). Δ*lytB* mutants are highly defective in cell separation and form long chains of unencapsulated cells (Table 1) (1, 15), but this striking phenotype is almost totally masked by capsule. Conversely, the absence of capsule led to less obvious defects in the cell shape and division of Δ*pmp23* mutants and again a defect in cell separation that caused chaining (Fig. 2). The difference in chaining characteristics of unencapsulated Δ*pmp23* mutants reported here and the lack of chaining in unencapsulated laboratory strain R6 reported before (45) may reflect the numerous mutations that have accumulated in strain R6 compared to its D39 progenitor (28). Some of these mutations drastically affect PG composition, resulting in extensive cross bridge formation in R6 that is largely absent in D39 (Fig. 1) (1). The mechanism underlying the link between capsule and effects on cell size and shape is unknown.

In addition, we identified the pneumococcal DacB L,D-carboxypeptidase for the first time and demonstrated that this enzyme is required for normal cell division in both capsulated and unencapsulated pneumococcal strains (Fig. 2). Bacterial L,D-carboxypeptidases fall into classes. Pa5198 of *Pseudomonas aeruginosa* and LdcA of *Escherichia coli* hydrolyze the peptide bond between D-Ala and L-*meso*-diaminopimelic acid in PG peptides and most likely function in PG recycling in the cytoplasm (27, 60). In contrast, pneumococcal $DacB_{Spn}$ contains a signal peptide and likely resides extracellularly as a lipoprotein. A homologue of *S. pneumoniae* DacB with 31% identical and 43% similar amino acids was previously identified in *L. lactis* (6). Similar to the Δ$dacB_{Spn}$ mutation reported here (Fig. 4), the Δ$dacB_{Lla}$ mutation caused increased or decreased relative amounts of the tetrapeptide or tripeptide PG monomers, respectively, in the PG of *L. lactis* (6). However, defects in cell division and decreased overall PG cross-linking were not reported previously for the Δ$dacB_{Lla}$ mutant (6, 49), in contrast to the phenotypes of the Δ$dacB_{Spn}$ mutant (Fig. 2 and 3). These phenotypic differences may somehow reflect the markedly different compositions of the PGs of *L. lactis* and *S. pneumoniae* strain D39, which contains D-Asp–D-Asn interpeptide cross bridges (45) or largely lacks L-Ala–L-Ser or L-Ala–L-Ala cross bridges (Fig. 1 and 4) (see reference 1), respectively.

Comparison of the PG lactoyl-peptide profiles and cell morphologies of combinations of Δ*dacB* and Δ*dacA* mutants in isogenic pneumococcus strains showed that the Δ*dacA* mutation is epistatic to the Δ*dacB* mutation (see Results). Mechanistically, this means that the DacA D,D-carboxypeptidase cleaves full-length pentapeptide PG monomers before the DacB L,D-carboxypeptidase and that tripeptide PG monomers, which are the product of the DacB L,D-carboxypeptidase, are largely absent in Δ*dacA* single mutants (Fig. 5). The roles of the D,D-carboxypeptidases in bacterial cell division are not fully understood (17, 38, 53, 66). These enzymes are tethered to the external surface of the cell membrane by a C-terminal amphipathic helix (see reference 53). A previous paper reported that $DacA_{Spn}$ localized everywhere in predivisional *S. pneumoniae* cells, except at equators (38). During later stages of PG biosynthesis, DacA became localized amorphously in midcell regions, and then following cell separation again appeared everywhere, except at equators. In a Δ*dacA* mutant, it was reported that the PBPs also became mislocalized relative to FtsZ (38). These combined results suggest that pneumococcal DacA is somehow occluded from equators at the start of cell division, thereby preserving the D-Ala–D-Ala-containing PG pentapeptides to direct the PBPs to proper division locations (38, 73). According to this model,

the PG-pentapeptide substrate localizes the pneumococcal PBPs, at least at early stages of division (73).

In contrast, the *E. coli* homologue of $DacA_{Spn}$, $PBP5_{Eco}$ (66), localized over entire lateral cell envelopes and concentrated at divisions sites, which contain PG-pentapeptide substrates and are actively carrying out PG biosynthesis (53). Our IFM localization results for both $DacA_{Spn}$ and $DacB_{Spn}$ (Fig. 6) strongly resemble those reported for $PBP5_{Eco}$ (53). As seen for $PBP5_{Eco}$, $DacA_{Spn}$ and $DacB_{Spn}$ localized in dense punctate patterns over the surfaces of cells in all stages of division (Fig. 6), instead of the smooth continuous patterns reported in reference 38. Gaps in localization indicative of occlusion were not detected at equators in this D39 strain, and $DacA_{Spn}$ and $DacB_{Spn}$ were concentrated at the septa of some dividing cells (Fig. 6). Our localization patterns are consistent with the conclusion reached for $PBP5_{Eco}$ (53) that recognition of PG pentapeptide substrate, which is detected at both equators and septa of wild-type pneumococcal cells by FL-V staining (Fig. 2), plays a role in directing the localization of $DacA_{Spn}$ and $DacB_{Spn}$.

The cell division defects caused by $\Delta dacB_{Spn}$ mutants (Fig. 2) suggest that the DacB L,D-carboxypeptidase also influences the availability of PG-peptide substrates used by PBPs for cross-linking. Tetrapeptide PG monomers accumulated in the PG of $\Delta dacB_{Spn}$ mutants, and the relative amount of cross-linked PG peptides decreased (Fig. 4). In addition, the PG of the $\Delta dacB_{Spn}$ mutant contained new cross-linked species, such as the D(*dacB*), not detected in the $dacB^+$ parent strain (Fig. 4A). Similar species containing extra D-Ala residues were detected previously in the PG of $\Delta dacB_{Lla}$ and $\Delta dacA_{Spn}$ mutants (6, 59). As proposed for $\Delta dacA_{Spn}$ mutants (38, 73), the cell division defects of $\Delta dacB_{Spn}$ mutants could again reflect mislocalization of PBPs caused by lack of normal PG-peptide substrates. Given that DacA D,D-carboxypeptidase and DacB L,D-carboxypeptidase carry out sequential reactions, an attractive hypothesis is that these proteins form a complex that promotes proper PBP localization and PG cross-linking. Although this work shows that DacA and DacB are the major carboxypeptidases in *S. pneumoniae* strain D39, minor peaks corresponding to the tripeptide and tetrapeptide PG monomer species were still present in the chromatograms of the Δ*dacA* Δ*dacB* double mutant (Fig. 5). The presence of these PG-peptide species likely arose through the activity of additional minor L,D-carboxypeptidases, whose identities, functions, and regulation remain to be determined.

Finally, this study supports the hypothesis that the $WalRK_{Spn}$ TCS regulon largely mediates PG hydrolysis in *S. pneumoniae* (Table 1). Essential PcsB and nonessential LytB and LysM protein Spd_1874 have been shown to act or be likely to act as PG hydrolases (see above; Table 1) (41, 42, 70). Protein Spd_0104 lacks an obvious hydrolase domain but is the only other protein, besides Spd_1874, that contains a LysM PG binding domain in *S. pneumoniae* strain D39. We show here that that the small (95-amino-acid) Spd_0703 protein is required for normal cell division (Fig. 2 and 3). Spd_0703, which contains an extended putative transmembrane region, has no homologues outside *Streptococcus* species. Δ*spd_0703* mutants formed normally shaped cells that stained aberrantly with FL-V (Fig. 2). Compared to the parent strains, FL-V staining of the Δ*spd_0703* mutants revealed prominent equatorial puncta, often skewed to one side of cells, pronounced banding at most septa, irrespective of invagination, and broadened equatorial puncta, especially in unencapsulated strains (Fig. 2). The composition of the PG peptides of the Δ*spd_0703* mutants was the same as that of the parent strain (Table 1). This result suggests that aberrant staining of the Δ*spd_0703* with FL-V was due to mislocalization, rather than an increased amount, of pentapeptide PG monomers in the PG. The likely membrane localization and PG peptide mislocalization phenotypes suggest that Spd_0703 is a new type of shape, elongation, division, and sporulation (SEDS) protein (see reference 21) that is conserved in *Streptococcus* species. The FL-V staining patterns suggest that Spd_0703 may be involved in early divisome or PG synthetic machinery placement, but mislocalization of the pentapeptide PG monomers in Δ*spd_0703* mutants is not severe enough to cause defective cell shapes. Future experiments will determine whether Spd_0703 interacts with other cell division or PG maturation proteins.

ACKNOWLEDGMENTS

We thank Adrian Land, Tiffany Tsui, and Krystyna Kazmierczak for discussions and comments about this work and Randy Arnold in the National Center for Glycomics & Glycoproteomics (NCGG) at Indiana University Bloomington for performing MS and tandem MS analyses.

This work was funded by grant 0543289 from the National Science Foundation and grant AI060744 from the National Institute of Allergy and Infectious Diseases to M. E. W. S. M. B. was a predoctoral trainee on NIGMS grant F31FM082090.

The contents of this paper are solely our responsibility and do not necessarily represent the official views of the granting agencies.

REFERENCES

1. **Barendt, S. M., et al.** 2009. Influences of capsule on cell shape and chain formation of wild-type and *pcsB* mutants of serotype 2 *Streptococcus pneumoniae*. J. Bacteriol. **191:**3024–3040.
2. **Bateman, A., and N. D. Rawlings.** 2003. The CHAP domain: a large family of amidases including GSP amidase and peptidoglycan hydrolases. Trends Biochem. Sci. **28:**234–237.
3. **Buist, G., A. Steen, J. Kok, and O. P. Kuipers.** 2008. LysM, a widely distributed protein motif for binding to (peptido)glycans. Mol. Microbiol. **68:**838–847.
4. **Cabre, M.** 2009. Pneumonia in the elderly. Curr. Opin. Pulm. Med. **15:**223–229.
5. **Chan, P. F., et al.** 2003. Characterization of a novel fucose-regulated promoter (P_{fcsK}) suitable for gene essentiality and antibacterial mode-of-action studies in *Streptococcus pneumoniae*. J. Bacteriol. **185:**2051–2058.
6. **Courtin, P., et al.** 2006. Peptidoglycan structure analysis of *Lactococcus lactis* reveals the presence of an L,D-carboxypeptidase involved in peptidoglycan maturation. J. Bacteriol. **188:**5293–5298.
7. **De Las Rivas, B., J. L. García, R. Lopez, and P. García.** 2002. Purification and polar localization of pneumococcal LytB, a putative endo-beta-*N*-acetylglucosaminidase: the chain-dispersing murein hydrolase. J. Bacteriol. **184:**4988–5000.
8. **den Blaauwen, T., M. A. de Pedro, M. Nguyen-Disteche, and J. A. Ayala.** 2008. Morphogenesis of rod-shaped sacculi. FEMS Microbiol. Rev. **32:**321–344.
9. **Dubrac, S., P. Bisicchia, K. M. Devine, and T. Msadek.** 2008. A matter of life and death: cell wall homeostasis and the WalKR (YycGF) essential signal transduction pathway. Mol. Microbiol. **70:**1307–1322.
10. **Dubrac, S., I. G. Boneca, O. Poupel, and T. Msadek.** 2007. New insights into the WalK/WalR (YycG/YycF) essential signal transduction pathway reveal a major role in controlling cell wall metabolism and biofilm formation in *Staphylococcus aureus*. J. Bacteriol. **189:**8257–8269.
11. **Eldholm, V., O. Johnsborg, K. Haugen, H. S. Ohnstad, and L. S. Håvarstein.** 2009. Fratricide in *Streptococcus pneumoniae*: contributions and role of the cell wall hydrolases CbpD, LytA and LytC. Microbiology **155:**2223–2234.
12. **Eldholm, V., et al.** 2010. Pneumococcal CbpD is a murein hydrolase that requires a dual cell envelope binding specificity to kill target cells during fratricide. Mol. Microbiol. **76:**905–917.
13. **Felmingham, D., R. Canton, and S. G. Jenkins.** 2007. Regional trends in beta-lactam, macrolide, fluoroquinolone and telithromycin resistance among *Streptococcus pneumoniae* isolates 2001–2004. J. Infect. **55:**111–118.
14. **Finn, R. D., et al.** 2010. The Pfam protein families database. Nucleic Acids Res. **38:**D211–D222.
15. **García, P., M. P. Gonzalez, E. García, R. Lopez, and J. L. García.** 1999. LytB, a novel pneumococcal murein hydrolase essential for cell separation. Mol. Microbiol. **31:**1275–1281.

16. **García-Bustos, J. F., B. T. Chait, and A. Tomasz.** 1987. Structure of the peptide network of pneumococcal peptidoglycan. J. Biol. Chem. **262:**15400–15405.
17. **Ghosh, A. S., C. Chowdhury, and D. E. Nelson.** 2008. Physiological functions of D-alanine carboxypeptidases in *Escherichia coli*. Trends Microbiol. **16:**309–317.
18. **Gillespie, S. H., et al.** 1997. Allelic variation in *Streptococcus pneumoniae* autolysin (*N*-acetyl muramoyl-L-alanine amidase). Infect. Immun. **65:**3936–3938.
19. **Gosink, K. K., E. R. Mann, C. Guglielmo, E. I. Tuomanen, and H. R. Masure.** 2000. Role of novel choline binding proteins in virulence of *Streptococcus pneumoniae*. Infect. Immun. **68:**5690–5695.
20. **Håvarstein, L. S., B. Martin, O. Johnsborg, C. Granadel, and J. P. Claverys.** 2006. New insights into the pneumococcal fratricide: relationship to clumping and identification of a novel immunity factor. Mol. Microbiol. **59:**1297–1307.
21. **Henriques, A. O., P. Glaser, P. J. Piggot, and C. P. Moran, Jr.** 1998. Control of cell shape and elongation by the *rodA* gene in *Bacillus subtilis*. Mol. Microbiol. **28:**235–247.
22. **Henriques-Normark, B., and S. Normark.** 2010. Commensal pathogens, with a focus on *Streptococcus pneumoniae*, and interactions with the human host. Exp. Cell Res. **316:**1408–1414.
23. **Izdebski, R., et al.** 2008. Highly variable penicillin resistance determinants PBP 2x, PBP 2b, and PBP 1a in isolates of two *Streptococcus pneumoniae* clonal groups, Poland 23F-16 and Poland 6B-20. Antimicrob. Agents Chemother. **52:**1021–1027.
24. **Job, V., et al.** 2003. Structural studies of the transpeptidase domain of PBP1a from *Streptococcus pneumoniae*. Acta Crystallogr. D Biol. Crystallogr. **59:** 1067–1069.
25. **Kadioglu, A., J. N. Weiser, J. C. Paton, and P. W. Andrew.** 2008. The role of *Streptococcus pneumoniae* virulence factors in host respiratory colonization and disease. Nat. Rev. Microbiol. **6:**288–301.
26. **Kausmally, L., O. Johnsborg, M. Lunde, E. Knutsen, and L. S. Håvarstein.** 2005. Choline-binding protein D (CbpD) in *Streptococcus pneumoniae* is essential for competence-induced cell lysis. J. Bacteriol. **187:**4338–4345.
27. **Korza, H. J., and M. Bochtler.** 2005. *Pseudomonas aeruginosa* LD-carboxypeptidase, a serine peptidase with a Ser-His-Glu triad and a nucleophilic elbow. J. Biol. Chem. **280:**40802–40812.
28. **Lanie, J. A., et al.** 2007. Genome sequence of Avery's virulent serotype 2 strain D39 of *Streptococcus pneumoniae* and comparison with that of unencapsulated laboratory strain R6. J. Bacteriol. **189:**38–51.
29. **Layec, S., B. Decaris, and N. Leblond-Bourget.** 2008. Characterization of proteins belonging to the CHAP-related superfamily within the Firmicutes. J. Mol. Microbiol. Biotechnol. **14:**31–40.
30. **Layec, S., B. Decaris, and N. Leblond-Bourget.** 2008. Diversity of Firmicutes peptidoglycan hydrolases and specificities of those involved in daughter cell separation. Res. Microbiol. **159:**507–515.
31. **Lechat, P., L. Hummel, S. Rousseau, and I. Moszer.** 2008. GenoList: an integrated environment for comparative analysis of microbial genomes. Nucleic Acids Res. **36:**D469–D474.
32. **Lopez, R., E. García, P. García, and J. L. García.** 2004. Cell wall hydrolases, p. 75–88. *In* E. I. Tuomanen, T. J. Mitchell, D. A. Morrison, and B. G. Spratt (ed.), The pneumococcus. American Society for Microbiology, Washington, D.C.
33. **Lynch, J. P., III, and G. G. Zhanel.** 2010. *Streptococcus pneumoniae*: epidemiology and risk factors, evolution of antimicrobial resistance, and impact of vaccines. Curr. Opin. Pulm. Med. **16:**217–225.
34. **Madeddu, G., A. G. Fois, P. Pirina, and M. S. Mura.** 2009. Pneumococcal pneumonia: clinical features, diagnosis and management in HIV-infected and HIV noninfected patients. Curr. Opin. Pulm. Med. **15:**236–242.
35. **Margolin, W.** 2009. Sculpting the bacterial cell. Curr. Biol. **19:**R812–R822.
36. **Maurer, P., et al.** 2008. Penicillin-binding protein 2x of *Streptococcus pneumoniae*: three new mutational pathways for remodelling an essential enzyme into a resistance determinant. J. Mol. Biol. **376:**1403–1416.
37. **Monterroso, B., J. L. Saiz, P. García, J. L. García, and M. Menendez.** 2008. Insights into the structure-function relationships of pneumococcal cell wall lysozymes, LytC and Cpl-1. J. Biol. Chem. **283:**28618–28628.
38. **Morlot, C., M. Noirclerc-Savoye, A. Zapun, O. Dideberg, and T. Vernet.** 2004. The D,D-carboxypeptidase PBP3 organizes the division process of *Streptococcus pneumoniae*. Mol. Microbiol. **51:**1641–1648.
39. **Morlot, C., A. Zapun, O. Dideberg, and T. Vernet.** 2003. Growth and division of *Streptococcus pneumoniae*: localization of the high molecular weight penicillin-binding proteins during the cell cycle. Mol. Microbiol. **50:**845–855.
40. **Musher, D. M., et al.** 2000. Bacteremic and nonbacteremic pneumococcal pneumonia. A prospective study. Medicine (Baltimore) **79:**210–221.
41. **Ng, W. L., K. M. Kazmierczak, and M. E. Winkler.** 2004. Defective cell wall synthesis in *Streptococcus pneumoniae* R6 depleted for the essential PcsB putative murein hydrolase or the VicR (YycF) response regulator. Mol. Microbiol. **53:**1161–1175.
42. **Ng, W. L., et al.** 2003. Constitutive expression of PcsB suppresses the requirement for the essential VicR (YycF) response regulator in *Streptococcus pneumoniae* R6. Mol. Microbiol. **50:**1647–1663.
43. **Ng, W. L., H. C. Tsui, and M. E. Winkler.** 2005. Regulation of the *pspA* virulence factor and essential *pcsB* murein biosynthetic genes by the phosphorylated VicR (YycF) response regulator in *Streptococcus pneumoniae*. J. Bacteriol. **187:**7444–7459.
44. **Nichols, R. J., et al.** 2011. Phenotypic landscape of a bacterial cell. Cell **144:**143–156.
45. **Pagliero, E., et al.** 2008. The inactivation of a new peptidoglycan hydrolase Pmp23 leads to abnormal septum formation in *Streptococcus pneumoniae*. Open Microbiol. J. **2:**107–114.
46. **Pagliero, E., et al.** 2004. Biochemical characterization of *Streptococcus pneumoniae* penicillin-binding protein 2b and its implication in beta-lactam resistance. Antimicrob. Agents Chemother. **48:**1848–1855.
47. **Pagliero, E., O. Dideberg, T. Vernet, and A. M. Di Guilmi.** 2005. The PECACE domain: a new family of enzymes with potential peptidoglycan cleavage activity in Gram-positive bacteria. BMC Genomics **6:**19.
48. **Pérez-Dorado, I., et al.** 2010. Insights into pneumococcal fratricide from the crystal structures of the modular killing factor LytC. Nat. Struct. Mol. Biol. **17:**576–581.
49. **Pérez-Núñez, D., et al.** 2011. A new morphogenesis pathway in bacteria: unbalanced activity of cell wall synthesis machineries leads to coccus-to-rod transition and filamentation in ovococci. Mol. Microbiol. **79:**759–771.
50. **Pinho, M. G., H. de Lencastre, and A. Tomasz.** 2000. Cloning, characterization, and inactivation of the gene *pbpC*, encoding penicillin-binding protein 3 of *Staphylococcus aureus*. J. Bacteriol. **182:**1074–1079.
51. **Pinho, M. G., and J. Errington.** 2003. Dispersed mode of *Staphylococcus aureus* cell wall synthesis in the absence of the division machinery. Mol. Microbiol. **50:**871–881.
52. **Piuri, M., and G. F. Hatfull.** 2006. A peptidoglycan hydrolase motif within the mycobacteriophage TM4 tape measure protein promotes efficient infection of stationary phase cells. Mol. Microbiol. **62:**1569–1585.
53. **Potluri, L., et al.** 2010. Septal and lateral wall localization of PBP5, the major D,D-carboxypeptidase of *Escherichia coli*, requires substrate recognition and membrane attachment. Mol. Microbiol. **77:**300–323.
54. **Ramos-Montañez, S., K. M. Kazmierczak, K. L. Hentchel, and M. E. Winkler.** 2010. Instability of *ackA* (acetate kinase) mutations and their effects on acetyl phosphate and ATP amounts in *Streptococcus pneumoniae* D39. J. Bacteriol. **192:**6390–6400.
55. **Reese, R. E., R. F. Betts, and B. Gumustop.** 2000. Handbook of antibiotics, third ed. Lippincott Williams & Williams, Philadelphia, PA.
56. **Rigden, D. J., M. J. Jedrzejas, and M. Y. Galperin.** 2003. Amidase domains from bacterial and phage autolysins define a family of gamma-D,L-glutamate-specific amidohydrolases. Trends Biochem. Sci. **28:**230–234.
57. **Robertson, G. T., W. L. Ng, J. Foley, R. Gilmour, and M. E. Winkler.** 2002. Global transcriptional analysis of *clpP* mutations of type 2 *Streptococcus pneumoniae* and their effects on physiology and virulence. J. Bacteriol. **184:** 3508–3520.
58. **Ronda, C., J. L. García, E. García, J. M. Sanchez-Puelles, and R. Lopez.** 1987. Biological role of the pneumococcal amidase. Cloning of the *lytA* gene in *Streptococcus pneumoniae*. Eur. J. Biochem. **164:**621–624.
59. **Severin, A., C. Schuster, R. Hakenbeck, and A. Tomasz.** 1992. Altered murein composition in a DD-carboxypeptidase mutant of *Streptococcus pneumoniae*. J. Bacteriol. **174:**5152–5155.
60. **Templin, M. F., A. Ursinus, and J. V. Holtje.** 1999. A defect in cell wall recycling triggers autolysis during the stationary growth phase of *Escherichia coli*. EMBO J. **18:**4108–4117.
61. **Tomasz, A., and W. Fischer.** 2006. The cell wall of *Streptococcus pneumoniae*, p. 230–240. *In* V. A. Fischetti, R. P. Novick, J. J. Ferretti, D. A. Portnoy, and J. I. Rood (ed.), Gram-positive pathogens, second ed. ASM Press, Washington, D.C.
62. **Tomasz, A., and W. Fischer.** 2000. The cell wall of *Streptococcus pneumoniae*, p. 191–200. *In* V. A. Fischetti, R. P. Novick, J. J. Ferretti, D. A. Portnoy, and J. I. Rood (ed.), Gram-positive pathogens. American Society for Microbiology, Washington, D.C.
63. **Typas, A., et al.** 2008. High-throughput, quantitative analyses of genetic interactions in *E. coli*. Nat. Methods **5:**781–787.
64. **van der Poll, T., and S. M. Opal.** 2009. Pathogenesis, treatment, and prevention of pneumococcal pneumonia. Lancet **374:**1543–1556.
65. **Vollmer, W., D. Blanot, and M. A. de Pedro.** 2008. Peptidoglycan structure and architecture. FEMS Microbiol. Rev. **32:**149–167.
66. **Vollmer, W., B. Joris, P. Charlier, and S. Foster.** 2008. Bacterial peptidoglycan (murein) hydrolases. FEMS Microbiol. Rev. **32:**259–286.
67. **Vollmer, W., and S. J. Seligman.** 2010. Architecture of peptidoglycan: more data and more models. Trends Microbiol. **18:**59–66.
68. **Walsh, C.** 2003. Antibiotics—actions, origin, resistance. ASM Press, Washington, D.C.
69. **Wayne, K. J., et al.** 2010. Localization and cellular amounts of the WalRKJ (VicRKX) two-component regulatory system proteins in serotype 2 *Streptococcus pneumoniae*. J. Bacteriol. **192:**4388–4394.
70. **Winkler, M. E., and J. A. Hoch.** 2008. Essentiality, bypass, and targeting of the YycFG (VicRK) two-component regulatory system in gram-positive bacteria. J. Bacteriol. **190:**2645–2648.
71. **Xu, Q., et al.** 2009. Structural basis of murein peptide specificity of a gamma-D-glutamyl-L-diamino acid endopeptidase. Structure **17:**303–313.
72. **Zapun, A., C. Contreras-Martel, and T. Vernet.** 2008. Penicillin-binding proteins and beta-lactam resistance. FEMS Microbiol. Rev. **32:**361–385.
73. **Zapun, A., T. Vernet, and M. G. Pinho.** 2008. The different shapes of cocci. FEMS Microbiol. Rev. **32:**345–360.